

# Ultrasonic Detection of Hydrogen Attack in Steels<sup>☆</sup>

A. S. Biring,\* M. L. Bartlett,\* and K. Kawano\*\*

## ABSTRACT

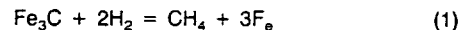
*Hydrogen attack is produced in steels from the seepage of hydrogen that reacts with carbides to form methane gas. This gas decarburizes the steel, produces microcracks, and lowers the toughness of the steel without necessarily a loss of thickness. Detection of hydrogen attack is important to assure safe operation of pressure vessels and piping susceptible to such damage. To nondestructively detect hydrogen attack, three ultrasonic techniques based on velocity, attenuation, and back-scatter, respectively, were investigated. Specifically, velocity decreased while attenuation and back-scattering increased. In samples with hydrogen attack, the experiments showed all three parameters were affected to a certain degree.*

*Based on this study, recommendations are that both velocity and back-scattering be used to detect hydrogen attack in steels. The study also determined that an inspection based only on velocity measurements may not detect earlier stages of hydrogen attack.*

## INTRODUCTION

Hydrogen attack is produced in steels exposed to high-pressure hydrogen at high temperatures.<sup>1</sup> Under such conditions, a chemical reaction occurs between hydrogen and steel to produce methane gas. The gas nucleates at the inside diameter (ID) grain

boundaries and progresses to the outside diameter (OD). Eventually, the nucleated cavity grows in size and merges into bubbles to form fissures. The kinetics of hydrogen attack depend on several variables<sup>1</sup> including temperature, pressure, and fluid flowing in the pipe. In general, the chemical reaction for hydrogen attack can be simplified to:



The formation of methane gas bubbles at the grain boundaries and the decarburization of the steel reduce the material's toughness without necessarily any reduction in thickness. This loss of structural strength from hydrogen attack has been known to produce several failures in petroleum<sup>2,3</sup> and fossil plants.<sup>4,5</sup>

To address the problem, in 1977, the American Petroleum Institute (API)<sup>(1)</sup> issued API Publication 941<sup>6</sup> that presents safe operating temperatures for various steels in hydrogen environments. Hydrogen damage was reported, however, in steel operating within the allowable temperatures, so a revision was published in 1983. Under the revised guidelines, some older equipment was found to be performing at unacceptably high temperatures. To guarantee continued safe operation, a proven nondestructive testing (NDT) technique for periodic assessment of hydrogen damage was needed.

For this purpose, ultrasonic techniques (UT) were investigated by the authors. The ultrasonic parameters under study included velocity, attenuation, and back-scatter measurements. Ul-

\*Submitted for publication July 1988; revised October 1988.

\*Southwest Research Institute, P.O. Box 28510, San Antonio, TX 78284.

\*\*Idemitsu Engineering Company, Chiba, Japan.

<sup>(1)</sup>American Petroleum Institute (API), Washington, DC.

trasonic tests were performed on steel samples containing hydrogen attack that were taken from piping and vessels previously in service in petrochemical plants. The tests showed that hydrogen attack decreased ultrasonic wave velocity and increased attenuation and back-scattering. A careful application of ultrasonic measurement techniques should, therefore, detect such damage.

### Background

Previous studies have already demonstrated that hydrogen attack changes the propagation of ultrasonic waves. A theoretical study performed by O'Connell and Budiansky<sup>7</sup> and Temple<sup>8</sup> showed that microcracks in a material affect the bulk modulus of elasticity and, thus, reduce the velocity of both longitudinal ( $v_l$ ) and shear ( $v_s$ ) waves. They also predicted that the decrease in velocity of longitudinal waves will be more than that of shear waves. Hence, hydrogen attack will increase the value of  $v_s/v_l$ . This result means that detection of hydrogen attack can be performed by measuring the ratio of transit time of longitudinal-to-shear waves ( $t_l/t_s = v_s/v_l$ ) without knowing the thickness. The theoretical results were found to be true by Birring, et al.,<sup>9</sup> Watanabe, et al.,<sup>10</sup> and Senior and Szilard.<sup>11</sup> Birring, et al.,<sup>9</sup> applied the velocity method to detect hydrogen attack in fossil-fired boiler tubes. Watanabe concluded that a steel is attacked by hydrogen if the ratio  $v_s/v_l$  is higher than 0.55. Normally, the value of the ratio is 0.54.

Another technique to detect hydrogen attack is measurement of attenuation. Loper, et al.,<sup>5</sup> applied ultrasonic attenuation to detect hydrogen attack in fossil-fired boiler tubes. An increase in attenuation by more than 3 decibel (db) across the thickness of a boiler tube [approximately 6.3-mm thick (0.25 in.)] was considered to be caused by hydrogen attack.

While ultrasonic velocity and attenuation techniques have been successfully applied, both have certain limitations. The velocity ratio technique works successfully when used to detect the last stages of hydrogen attack and when hydrogen attack has produced a uniform porosity (microcracks) in the material, which reduces the velocity, but the technique may not be able to detect isolated porosity.

The attenuation technique works very well if the surface of the component on the side opposite to the transducer is smooth (e.g., smooth ID surface when the transducer is placed on a smooth area of the OD surface). The reliability of the attenuation technique deteriorates sharply on rough surfaces that scatter ultrasound.

In this study, the authors investigated ultrasonic velocity, attenuation, and back-scatter techniques on samples known to have hydrogen attack. As just discussed, all previous work for hydrogen attack detection had been limited to velocity and attenuation; the back-scatter technique had not been used for such an application. Back-scatter had been limited primarily to grain-size determination in the field of NDT.

## EXPERIMENTAL TESTS

### Samples

Ultrasonic tests were conducted on two samples received from two petroleum-related confidential sources. One set of five samples, supplied from one source and identified as Set A, was cut from a pipe with a 16.8-cm (6.625-in.) OD and 1.8-cm (0.718-in.) thickness. Four of the samples (A-1 through A-4) with hydrogen attack were cut from 90-, 180-, 270-, and 360-degree locations of the pipe, respectively. The fifth sample (A-5) was from another pipe location with no hydrogen attack. A second set of samples, identified as Set B, was cut from a 98-mm- (3.85-in.)-thick vessel made out of ASTM<sup>(2)</sup> A204 Grade A steel. Three samples were made (B-1 through B-3); each sample was a 25-mm-

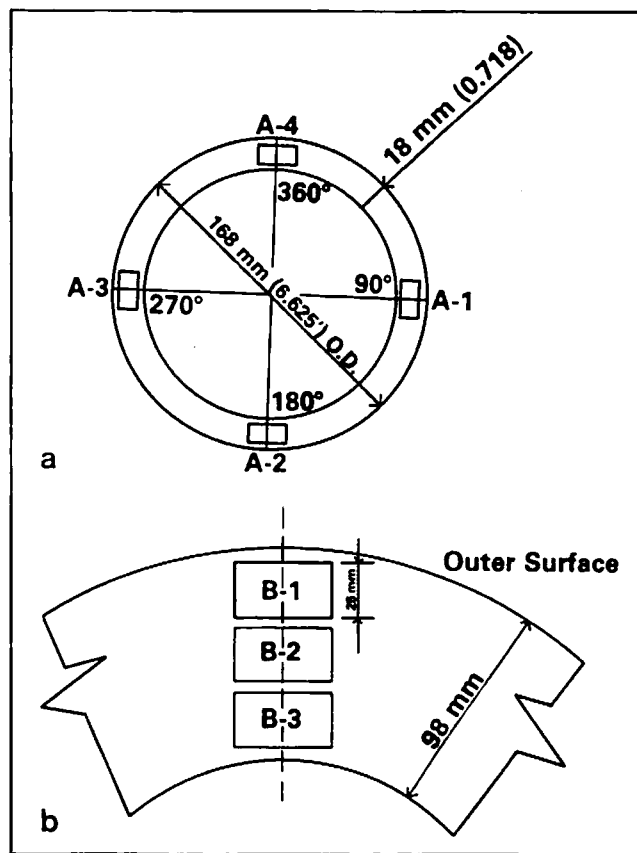


FIGURE 1. Schematic illustration of sample locations taken from a pipe (Set A) and a vessel (Set B). (a) Samples A-1 through A-4 with hydrogen attack were cut at the same axial location on the pipe. Sample A-5 was cut from the same pipe, but at a different axial location with no hydrogen attack. (b) Samples B-1 through B-3 were cut through the outside surface, midthickness, and inside surface of the vessel, respectively.

(1-in.)-thick piece cut across the thickness of the vessel wall from the OD through the ID (see Figure 1).

### Material Tests

Metallurgical investigations were performed on the samples to verify that they had hydrogen attack. Metallography was performed on all the samples to detect microcracks. Additional tests that included measurements of fracture toughness were performed on sample Set B.

**Metallography** — Hydrogen attack in the specimens was confirmed by metallography. Micrographs taken on Samples A-1 through A-4 showed microcracking and decarburization. Figure 2(a) shows the micrograph (4X magnification) for Sample A-2 (180 degrees) in which two-thirds of the thickness from the ID was attacked by hydrogen. Microcracks and decarburization are visible (200X magnification), as shown in Figure 2(b). The microcracks at the ID were approximately 50  $\mu\text{m}$ . Metallurgical investigation revealed the hydrogen attack in Set A was in an advanced stage. A micrograph of Sample B-3 (ID) (see Figure 3) displayed cracks of the order of 25  $\mu\text{m}$  produced by hydrogen attack. Metallurgical investigations showed isolated microcracks on a few grain boundaries in Sample B-3 compared to Samples A-1 through A-4 and established that the hydrogen attack in Sample B-3 was in an early stage. No hydrogen attack was evident at the OD (Sample B-1).

**Charpy Impact Tests** — To obtain absorbed energy measurements, 2-mm V-notch Charpy impact tests were taken on sample

<sup>(2)</sup>ASTM, Philadelphia, Pennsylvania.

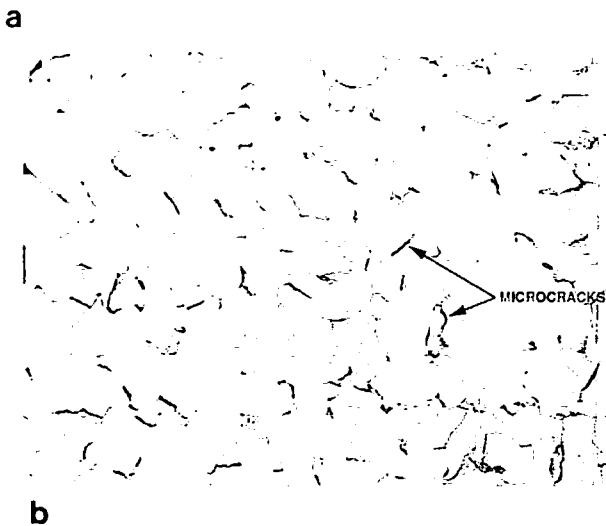
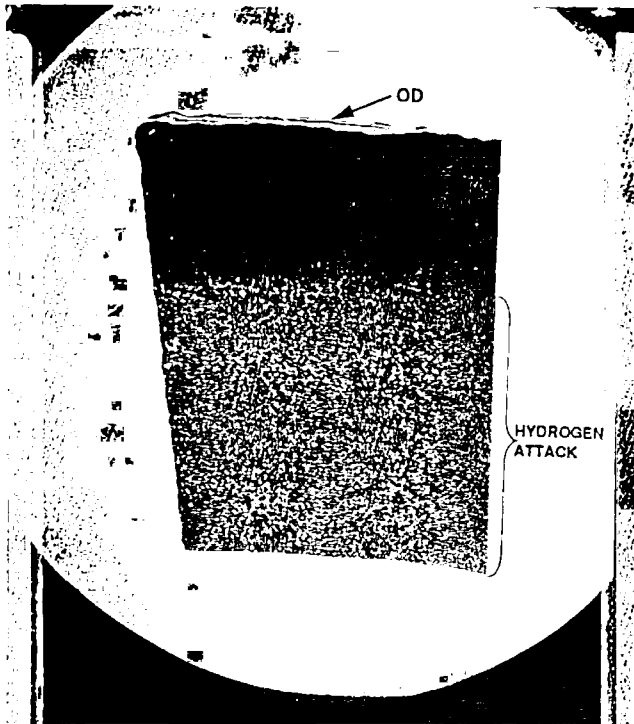


FIGURE 2. Micrographs showing hydrogen attack in Set A samples. (a) Sample A-2 shows damage through about two-thirds of its thickness. (b) Microcracks, about 50- $\mu\text{m}$  long, are shown at the inside surface.

Set B using a 294-joules (J) testing machine. The absorbed energy value registered lower in specimens at the ID and mid-thickness compared to the OD, demonstrating that hydrogen attack was present in up to two-thirds of the metal thickness from the ID. The value of the absorbed energy dropped from 40 J for Specimen B-1 at the OD to 25 J for Specimen B-2 at the mid-thickness and to 24 J for Specimen B-3 at the ID (see Table 1).

**Fracture Toughness** — Fracture toughness ( $K_{Ic}$ ) measurements were taken on Samples B-1 and B-3. These tests were performed to verify hydrogen attack as the micrographs showed very few microcracks in Sample B-3. The metallographs of Sample B-3 showed some evidence of hydrogen attack, but the fracture toughness test was used for further verification.

Toughness was characterized using  $J_{Ic}$ , an elastic-plastic toughness parameter, and  $K_{Ic}$ . Specimens B-1 and B-3 were tested to assess the inherent variability in this property. The experimental procedure followed the standard test method of ASTM

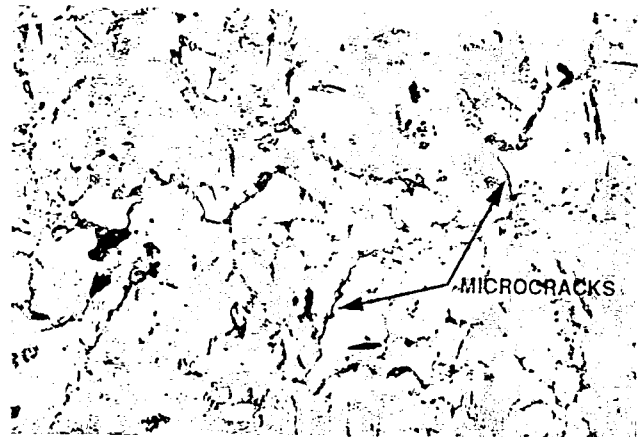


FIGURE 3. Micrographs showing hydrogen attack in Sample B-3. Early stages of hydrogen attack were detected in this sample.

TABLE 1  
Absorbed Energy Measured by the 294-J Charpy  
Test Machine and Fracture Toughness Values ( $K_{Ic}$ )  
Characterized Using  $J_{Ic}$ , an Elastic-Plastic Toughness Parameter

Sample No.	Location	Absorbed Energy (J)	$K_{Ic}$ (MPa $\sqrt{\text{m}}$ )
B-1	outside diameter	40	134.1
B-2	midthickness	25	test malfunction
B-3	inside diameter	24	76.1

E813<sup>12</sup> and ASTM E399<sup>13</sup> for measuring fracture toughness. The specimens used were the standard compact-type (CT) in ASTM E399, with a hole drilled at the end of the notch to facilitate easy placement of the clip gage on the created ledges. This procedure generated a J-resistance curve (increase in toughness as a function of crack growth). Crack extension was monitored using elastic compliance techniques.<sup>12,13</sup> The compliances were obtained from load displacement slopes, measured during periodic unloadings. The J-integral was determined and then plotted against physical crack growth.

Fracture toughness values were calculated from the measurements taken during the tests. The results, given in Table 1, showed that the value of fracture toughness at the ID was 57% of the value at the OD of the specimen. This decrease was attributed to hydrogen attack.

While the two  $J_{Ic}$  tests were performed on one sample (one test from the OD and one from the ID), the results should still be statistically valid. (Only single samples were used because of limited availability.) This was because the  $J_{Ic}$  test was performed by applying several load excursions (10 to 20) on a single sample. The data obtained from these excursions were extrapolated to obtain  $J_{Ic}$ , which was used to calculate  $K_{Ic}$ .

### Ultrasonic Measurements

Results of the ultrasonic velocity, attenuation, and backscatter measurement tests conducted on the hydrogen attack samples are discussed in the following subsections.

**Velocity** — Velocity measurements were taken on both sets of samples using the pulse-echo (reflection) overlap technique. Both longitudinal- and shear-wave measurements were made in the radial direction. Measurements for Set A samples, given in Table 2, showed that the longitudinal-wave velocity decreased by 7 to 11% relative to the velocity in Sample A-5 (without hydrogen attack), while the shear-wave velocity decreased by 3 to 6% relative to the velocity in Sample A-5. The ratio of  $v_s/v_l$  for Samples

TABLE 2  
Longitudinal- and Shear-Wave Velocity  
Measurements Taken at an Ultrasonic Frequency of 5 MHz

Sample No.	Location (degrees)	Velocity ( $\times 10^6$ mm/sec)			
		$v_l$	$\Delta v$ (percentage)	$v_s$	$\Delta v$ (percentage)
A-1	90	5.33	-9.3	3.10	-3.1
A-2	180	5.46	-7.1	3.08	-3.7
A-3	270	5.37	-8.6	3.01	-5.9
A-4	360	5.28	-10.2	3.06	-4.4
A-5	( <sup>1</sup> )	5.88	0	3.20	0
B-1	outside surface	5.91	0	3.250	0
B-2	midsection	5.87	-0.7	3.233	-0.5
B-3	inside surface	5.84	-1.2	3.227	-0.7

(<sup>1</sup>) Sample with no hydrogen attack.

A-1 through A-4 damaged by hydrogen attack ranged from 0.56 to 0.58, and the ratio on Sample A-5 was 0.544. These results are in direct agreement with the results of Reference 10.

The results of velocity measurements on the three samples in Set B, given in Table 2, showed a very small decrease in velocity compared to samples in Set A. The longitudinal-wave velocity decreased by only 1% at the ID compared to the OD, which had no hydrogen attack. The shear-wave velocity decreased by 0.7% compared to the OD. The ratio  $v_s/v_l$  increased by a very small amount from 0.550 at the OD to 0.553 at the ID, even though there was significant difference in the amount of hydrogen attack. Sample B-1 (OD) showed no microcracks, while Sample B-3 (ID) showed microcracking.

**Attenuation** — Attenuation measurements were taken on both sets of samples. Results from Set A, taken at 10 MHz (see Table 3), showed that attenuation in the hydrogen attack samples was 4.2 to 5.8 db/cm, and 1.6 db/cm in the sample not attacked by hydrogen — clearly demonstrating that attenuation increases with hydrogen attack. Results of attenuation on Set B, given in Table 3, showed that attenuation increased from 1.7 db/cm at the OD to 3.2 db/cm at the ID, which had hydrogen attack.

**Back-Scatter** — Ultrasonic back-scatter is a method in which the ultrasonic waves scattered from within a material are analyzed. Figure 4 shows the concept of measuring back-scattered signals. Back-scattering occurs from the grains because of impedance mismatch at the material's grain boundaries. Back-scattering increases with frequency, so these measurements are usually conducted at high frequencies such as 10 MHz.

Results of back-scatter on the samples in Set A, given in Table 4, show that the back-scatter amplitude (relative) increased from 2 mV in the sample with no hydrogen attack to an amplitude range of 13 to 24 mV on samples attacked by hydrogen. Results of back-scatter measurements on samples in Set B, given in Table 4, showed that the back-scatter amplitude increased from 2 mV at the OD, where there is practically no hydrogen, to 20 mV at the ID. Figure 5 presents the oscilloscope traces of the amplitude at the OD and ID, which definitely show the strong increase in back-scatter at the ID.

## DISCUSSION OF RESULTS

The velocity, attenuation, and back-scatter measurements on both sets of specimens demonstrated that all three parameters were affected by hydrogen attack. The most significant results were obtained on Set B samples, which had low levels of hydrogen attack compared to Set A. Because the velocity measurements on Set B samples displayed a very small decrease (1%), the conclusion based only on the velocity measurement could be reached that the B-3 sample had no damage. The ratio of  $v_s/v_l$  at the ID was also only 0.553, even though the sample had damage. Attenuation measurements showed a definite increase from 1.7 db

TABLE 3  
Attenuation Measurements Taken at an  
Ultrasonic Frequency of 10 MHz

Sample No.	Location (degrees)	Relative Attenuation (db/cm)
A-1	90	4.2
A-2	180	5.8
A-3	270	5.0
A-4	360	5.3
A-5	( <sup>1</sup> )	1.6
B-1	outside diameter	1.7
B-2	midthickness	2.4
B-3	inside diameter	3.2

(<sup>1</sup>) Sample with no hydrogen attack.

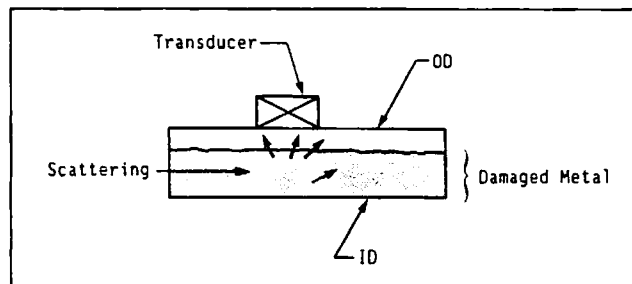


FIGURE 4. Test configuration to measure ultrasonic back-scattering caused by discontinuities within the material.

at the OD to 3.2 db at the ID, which could indicate damage. Attenuation measurements, however, can result in false indications if the ID surface is pitted and scatters ultrasound. The most prominent results on the samples in Set B were determined from the back-scatter measurements, which displayed a significant increase in amplitude at the ID — about 10 times over the OD.

The back-scattering result is very important since it was found to be more sensitive to detect hydrogen attack on sample Set B compared to velocity measurements. Taking only velocity measurements on Sample B would have led to an incorrect conclusion that Sample B-3 had experienced no hydrogen attack.

The difference between the velocity and back-scatter is caused because they are affected by two different material parameters. Velocity reduction is caused by an overall decrease in the bulk modulus of elasticity (in the metal volume) caused by microcracking.<sup>7</sup> Such a decrease in bulk modulus is produced when a large number of microcracks are present or the material has extensive hydrogen attack. Back-scattering, on the other hand, is caused by impedance mismatch at grain boundaries in the material.

TABLE 4  
Relative Back-Scatter Signal Amplitudes Taken  
at an Ultrasonic Frequency of 10 MHz

Sample No.	Location (degrees)	Back-Scatter Amplitude (mV)
A-1	90	13
A-2	180	24
A-3	270	14
A-4	360	14
A-5	(1)	2
B-1	outside surface	2
B-2	midsection	15
B-3	inside surface	20

(1) Sample with no hydrogen attack.

While the back-scattering method is sensitive to cavities and microcracks produced by hydrogen attack, the technique has to be used carefully to avoid erroneous results. Back-scattering measurements can sometimes be misleading since other factors such as anisotropy between grains or the boundary of two different metallic phases in an alloy can produce back-scattering. To account for such effects, back-scattering measurements taken on a component being inspected should always be compared to another location (reference) on the same component with no hydrogen attack. The difference between the two back-scatter measurements will result from hydrogen attack. This is similar to comparing the measurements of Specimen A-1 to Specimen A-5 (see Table 4).

The major advantage of using back-scatter measurements to determine hydrogen attack is that the technique analyzes only the sound scattered within the material and is not affected by the condition of the ID surface. In fact, back-scatter measurements can be taken on geometries that do not produce a back-surface reflection required by velocity and attenuation measurements.

## CONCLUSIONS

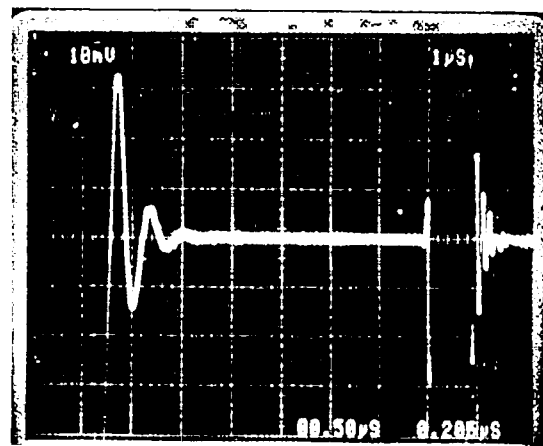
Since hydrogen attack undetected in certain components can cause serious consequences, a reliable nondestructive approach is essential. Three nondestructive techniques using velocity, attenuation, and back-scatter approaches were applied on samples to detect and measure hydrogen attack. Ultrasonic longitudinal-wave velocity was found to decrease by almost 10% in one of the samples; however, this was not true for another sample, which only showed a 1% decrease. The ultrasonic back-scatter technique was more sensitive to detecting hydrogen attack, as indicated by an increase of back-scatter signal amplitudes by almost 10 times on samples with attack degradation. The back-scatter technique is also better than the attenuation technique, which is affected by surface roughness at the ID and requires a back-surface reflection. To reliably determine the internal condition of materials, both back-scatter and velocity measurements should be taken.

## ACKNOWLEDGMENTS

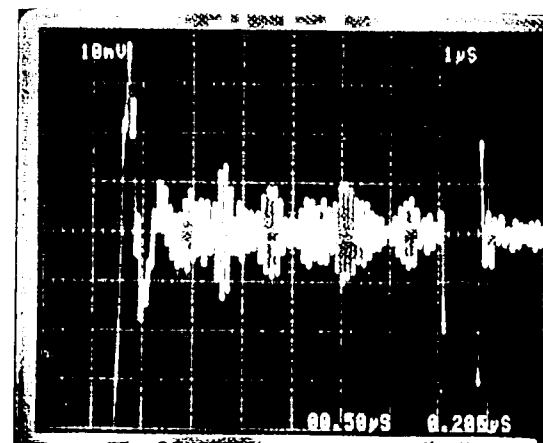
The authors wish to acknowledge the assistance of G. Hendrix, D. G. Alcazar, and J. Hanley in taking ultrasonic measurements.

## REFERENCES

1. P. G. Shewmon, *Met. Trans. A*, Vol. 7A, pp. 279-286, February 1976.
2. R. D. Merrick, A. R. Ciuffreda, "Hydrogen Attack of Carbon-0.5 Mo Steel—Are the Present Limits Acceptable?," Paper No. 100, CORROSION/82, NACE, Houston, Texas, 1982.
3. A. R. Ciuffreda, D. R. Rowland, "Hydrogen Attack of Steel in Reformers Service," Proc. Twenty-Second API Mid-Year Meeting, Vol. 37 (III), American Petroleum



a



b

FIGURE 5. Back-scattering from hydrogen-attack measurements using a 10-MHz transducer. (a) Back-scattering from Sample B-1 cut from the outside surface with no hydrogen attack. (b) Back-scattering from Sample B-3 cut from the inside surface, which had hydrogen attack.

- Institute (API), New York, New York, pp. 116-128, 1957.
4. E. P. Partridge, *J. Engineering for Power*, Trans. ASME, Paper No. 63-PWR-9, American Society of Mechanical Engineers (ASME), New York, New York, 1963.
5. M. H. Loper, R. D. Shoemaker, J. A. Strump, "Mitigating Forced Outages by Selective Replacement of Boiler Tubes," Proc. of the EPRI Conf. on Failures and Inspection of Fossil Fired Boiler Tubes, Electric Power Research Institute (EPRI) CS-3272, Palo Alto, California, pp. 6-35 to 6-52, April 1983.
6. API Publication 941, "Steel for Hydrogen Service at Elevated Temperatures and Pressures in Petroleum Refineries and Petrochemical Plants," API, Washington, DC (June 1977) (revised, 1983 3rd edition).
7. R. J. O'Connell, B. Budiansky, *J. Geophysical Research*, Vol. 82, No. 36, pp. 5719-5735, December 1977.
8. J. A. G. Temple, "Developments in Theoretical Modeling for Ultrasonic NDT," Harwell Report No. TP.1143, Harwell Laboratory, Oxfordshire, UK, July 1985.
9. A. S. Biring, D. G. Alcazar, J. J. Hanley, G. J. Hendrix, S. Gehl, "Detection of Hydrogen Damage by Ultrasonics," Proc. the EPRI Conference on Boiler Tube Failures in Fossil Plants, EPRI CS-5500SR, EPRI, Palo Alto, California, 1987.
10. T. Watanabe, T. Hasagawa, K. Kato, "Ultrasonic Velocity Ratio Method for Detecting and Evaluating Hydrogen Attack in Steels," *Corrosion Monitoring in Industrial Plants Using Nondestructive Testing and Electrochemical Methods*, American Society for Testing and Materials (ASTM) STP 908, Philadelphia, Pennsylvania, pp. 153-164, August 1986.
11. P. Senior, J. Szilard, *Ultrasonics*, pp. 42-44, January 1984.
12. ASTM Standard Test Method for  $J_{IC}$ , "A Measure of Fracture Toughness," 1986 Annual Book of ASTM Standards, ASTM E 813-81, ASTM, Philadelphia, Pennsylvania, pp. 768-786, 1986.
13. ASTM Standard, "Test Method for Plane-Strain Fracture Toughness of Metallic Materials," 1986 Annual Book of ASTM Standards, ASTM E 399, ASTM Philadelphia, Pennsylvania, pp. 522-557, 1986.